Theoretical study of the hydrated Gd3+ ion: Structure, dynamics, and charge transfer

C. Clavaguéra, Florent Calvo, J.-P. Dognon

Theoretical study of the hydrated Gd^{3+} ion: structure, dynamics and charge transfer

Carine Clavaguéra, Florent Calvo[a)], Jean-Pierre Dognon[*]

Theoretical Chemistry Laboratory DSM/DRECAM/SPAM-LFP (CEA-CNRS URA2453)

CEA/SACLAY, Bat.522, 91191 GIF SUR YVETTE, FRANCE

Abstract

The dynamical processes taking place in the first coordination shells of the gadolinium (III) ion are important for improving the contrast agent efficiency in magnetic resonance imaging. An extensive study of the gadolinium (III) ion solvated by a water cluster is reported, based on molecular dynamics simulations. The AMOEBA force field [J. Phys. Chem. B **107**, 5933 (2003)] that includes many-body polarization effects is used to describe the interactions among water molecules, and is extended here to treat the interactions between them and the gadolinium ion. In this purpose accurate *ab initio* calculations have been performed on Gd^{3+}-H_2O for extracting the relevant parameters. Structural data of the two first coordination shells and some dynamical properties such as the water exchange rate between the first and second coordination shell are compared to available experimental results. We also investigate the charge transfer processes between the ion and its solvent, using a fluctuating charges model fitted to reproduce electronic structure calculations on $[Gd(H_2O)_n]^{3+}$ complexes, with n ranging from 1 to 8. Charge transfer is seen to be significant (about one electron) and correlated with the instantaneous coordination of the ion.

[a)] Permanent address: Laboratoire de Physique Quantique, IRSAMC, Université Paul Sabatier, 118 Route de Narbonne, F31062 TOULOUSE CEDEX, FRANCE

[*] Corresponding author: Jean-Pierre Dognon, jean-pierre.dognon@cea.fr

I- Introduction

The number of water molecules involved in a hydrated gadolinium (III) complex notably determines the efficiency of the contrast agent used in magnetic resonance imaging (MRI) for medical diagnosis.[1] In MRI the hydrogen atoms of the water molecules need to be close to the Gd^{3+} ion to enhance proton spin relaxation. At the present time, commercial agents contain only one water molecule complexed simultaneously to the gadolinium ion with an organic ligand. Challenging investigations are being carried out to find efficient complexes with two water molecules,[2] however and up to now, no such system that is stable and could be immediately usable has been reported yet. Another trend of research is dynamical and consists in optimizing the exchange rate of the water molecules to improve the efficiency of the contrast agents.[2]

Molecular modeling and explicit force fields can help to better understand the local complexation properties of the gadolinium ion and to provide grounds for the development of new optimized ligands. The use of molecular simulation is justified by the need for statistical and dynamical properties, the presence of rather rare events taking place over hundreds of picoseconds in explicit water.

Recent studies have shown that a great care should be paid to the force field used to model such systems in order to get consistent structural and dynamical properties along the lanthanide series.[3,4,5] The AMOEBA force field[6,7] developed by Ren, Ponder and coworkers presently stands as one of the most accurate force field available for water. It has previously been used successfully to determine solvation free energies for K^+, Na^+ and Cl^- ions in liquid water and formamide[6] and to investigate the role of polarization effects in alanine dipeptide.[8] More recently, it was used in the Jungwirth group to elucidate the propensity of heavier halides for being located near the water/vapor interface.[9]

The present article focuses on the solvation dynamics of the gadolinium ion, in order to determine the properties of the first coordination shells of this ion. The AMOEBA framework was chosen for several reasons. First, its performances in reproducing cluster, liquid and solid bulk

properties are particularly good,[7] and its numerical cost remains relatively modest. More importantly in the present context, and contrary to most conventional force fields, the AMOEBA force field incorporates important physical interactions such as self-consistent polarization forces, which turn out to be critical for the present solvated ion.[5]

Extending AMOEBA to treat the lanthanide ion requires accurate estimation of its interaction with water molecules. Reference calculations, performed at relativistic *ab initio* levels, are thus required in order to extract the relevant parameters in the force field.

Another motivation of the present work is to look at charge transfer (CT) between the ion and the nearby solvent molecules. Indeed for lanthanide (III) ions, it could be expected that the polarization term does not completely represent all the many-body effects. In the AMOEBA force field framework, charge transfer is not explicitly taken into account but implicitly included via the parameters derived from *ab initio* calculations that obviously contain all these effects. The purpose of this preliminary study is to evaluate the order of magnitude of the charge transfer in the case of lanthanide (III) complexes. While CT can be conveniently estimated from first-principles calculations, most conventional force fields assume for simplicity that the partial charges carried by the atoms remain fixed. This approximation is obviously doubtful for highly flexible systems, and a number of improved force fields that account for these effects have appeared. Here we have used the fluctuating charges (fluc-q) framework first introduced by Mortier and coworkers[10] and by Rappé and Goddard[11], also known as the charge equilibration method. Fluc-q models have become widespread in chemical physics and condensed matter physics. Illustrative applications of fluctuating charges models include liquid water,[12] ionic melts,[13] metal oxydes,[14] heterogeneous clusters,[15] and more recently biomolecules.[16] Fluctuating charges are also a key part of reactive potentials such as ReaxFF.[17]

AMOEBA assumes a set of fixed partial charges, which only interact when they belong to *different* molecules. Charge transfer mainly takes place along chemical bonds within each molecule, with a lesser influence from the environment. Such intramolecular interactions are precisely

needed in fluc-q potentials, hence there is a fundamental incompatibility between the current implementation of AMOEBA and fluctuating charges. Thus it does not seem appropriate to incorporate fluctuating charges in AMOEBA, as this would alter all other polarization effects. Nevertheless fluc-q models remain very useful to estimate charge transfer in large systems, because they rely on well defined approximations to electronic structure theory,[18] through Sanderson's principle of electronegativity equalization.[19] As a result, these models can be taught to mimic first-principle data, and transferred to more complex systems out of reach at the *ab initio* level. Thus fluc-q models provide a relatively inexpensive but quite accurate way of quantifying the various effects of charge transfer in the solvated system containing hundreds of atoms. In the present work, a fluc-q model has been parametrized on our electronic structure calculations as a tool for processing the trajectories generated using AMOEBA.

The paper is organized as follows. In the next Section, we briefly recall the main elements of the AMOEBA force field, and its extension to the gadolinium (III) ion. We also briefly give details about the conditions under which the simulations were performed. In Section III, the structure of the first and second coordination shells of the gadolinium ion in a cluster of 120 water molecules is discussed. An analysis of the residence time of the water molecules in the first shell is given. Section IV is devoted to the charge transfer effects, and includes the *ab initio* reference calculations performed on small clusters and a short description of the fluc-q model. We analyse the molecular dynamics trajectories in terms of the charge transferred to the gadolinium ion, paying a particular attention to its correlation with the coordination and the related water exchange phenomena. We finally summarize and conclude in Sec. V.

II- Molecular modeling using AMOEBA

a. The AMOEBA force field

The AMOEBA force field[7] was chosen here because of its reliability to reproduce many water properties, including the dipole moment of gas phase H_2O and the liquid dielectric

constant. The ideas behind AMOEBA consist in modeling intermolecular forces with a high-level model potential fitted to *ab initio* data only, that is without introducing any experimental data. The analytical form of the force field is based on the second-order exchange-perturbation theory of intermolecular forces.

The electrostatic component incorporates not only a fixed partial charge, but also a dipole and a quadrupole on each atom as derived from quantum mechanical calculations in a Stone's distributed multipole analysis framework (GDMA program[20]).

Many-body polarization effects are explicitly treated using a self-consistent dipole polarization procedure. The induced dipole on each site *i* is written:

$$\mu_{i,\alpha}^{ind} = \alpha_i E_{i,\alpha} \quad \left(\alpha \in \{x,y,z\}\right) \quad (1)$$

with α_i the atomic polarizability and $E_{i,\alpha}$ the electric field on atom *i*.

As a result,

$$\mu_{i,\alpha}^{ind} = \alpha_i \sum_{\{j\}} T_{\alpha}^{i,j} M_j + \alpha_i \sum_{\{j'\}} T_{\alpha\beta}^{i,j'} \mu_{j',\beta}^{ind} \quad (2)$$

with *T* the usual interaction matrix and M_j contains the permanent multipole components.

The first term in Eq. (2) represents the dipole on site *i* induced by the permanent multipoles of the other molecules. The second term represents the dipole on site *i* induced by the other induced dipoles.

A polarization-damping scheme[21] is used to avoid polarization catastrophe at short distances. A smeared charge distribution replaces the point dipoles with the form:

$$\rho = \frac{3a}{4\pi}\exp\left(-au^3\right) \quad \text{with} \quad u = R_{ij} \Big/ \left(\alpha_i \alpha_j\right)^{1/6} \quad (3),$$

u is the effective distance as a function of atomic polarizabilities between sites *i* and *j*, *a* is a dimensionless width parameter of the smeared charge distribution which controls the strength of damping (*a* was set to 0.39 for the water AMOEBA force field[7]).

Repulsion-dispersion interactions between pairs of nonbonded atoms are represented by a buffered 14-7 potential:

$$U_{ij}^{Buff} = \varepsilon_{ij}\left(\frac{1+\delta}{\rho_{ij}+\delta}\right)^{n-m}\left(\frac{1+\gamma}{\rho_{ij}^{m}+\gamma}-2\right) \quad (4)$$

where ε_{ij} is the potential well depth, $\rho_{ij} = R_{ij}/R_{ij}^{o}$ (R_{ij}^{o} the equilibrium energy distance, n = 14, m = 7, δ = 0.07 and γ = 0.12. For heterogeneous atoms pairs, the following combining rules were used:

$$R_{ij}^{o} = \frac{R_{ii}^{o\,3} + R_{jj}^{o\,3}}{R_{ii}^{o\,2} + R_{ii}^{o\,2}} \; and \; \varepsilon_{ij} = \frac{4\varepsilon_{ii}\varepsilon_{jj}}{(\varepsilon_{ii}^{1/2} + \varepsilon_{ii}^{1/2})^{2}} \quad (5)\ .$$

This buffered 14-7 potential is known to reproduce simultaneously series of *ab initio* results in gas phase and liquid properties on noble gas and diatomic species, with a better accuracy than the usual 12-6 Lennard-Jones pair potential.[22]

We plan in the future to study the complexation of the Gd^{3+} ion with a highly flexible organic ligand. In anticipation, the water molecules have been considered here as flexible. The intramolecular valence terms consist in bond stretching, angle bending and torsion, all being taken from the MM3 force field.[23] Furthermore, anharmonicity effects are added through the use of higher-order deviations from ideal bond lengths and angles. Additional valence terms are used to model the coupling between stretching and bending, with an Urey-Bradley functional form.

b. Extending AMOEBA to the gadolinium (III) ion

The AMOEBA parameters for Gd^{3+} ion were obtained from *ab initio* calculations performed at the CCSD(T) / LC-ECP+CPP (large core effective core potential associated to a core polarization potential) level[24,25] with uncontracted basis sets, energetically corrected from basis set superposition error (BSSE). The gadolinium repulsion-dispersion parameters were fitted from a sample of configurations (about 50) of the Gd^{3+}-H_2O dimer to sample the potential energy surface by varying the Gd-O distance and the orientation of the water molecule (ε_{Gd} = 10.0 kcal/mol and R_{Gd} = 3.65 Å).

From our experience, a good transferability of the parameters to larger water-gadolinium clusters is expected thanks to the accuracy of the reference *ab initio* data.[5,26] In addition, the dipole polarizability α_{Gd} of Gd^{3+} was determined with the same method as previously validated by all-electron fully relativistic 4-component Dirac Hartree-Fock calculations.[25] The value of α_{Gd} for the model potential was set to 0.790 $Å^3$.

c. Simulation details

Initial configurations of the $[Gd(H_2O)_{120}]^{3+}$ clusters were generated with the Solvate program.[27] Water molecules fill a defined solvent volume around the ion, one molecule after another based on steric criteria. Each structure wass optimized with a steepest descent procedure to obtain an energetically favorable position, considering only van der Waals energies. For propagation of dynamical trajectories, the integration method we used was the Beeman algorithm.[28] Molecular dynamics simulations were performed at constant temperature with a Berendsen thermostat.[29] The water-gadolinium cluster was confined by spherical boundary conditions with a van der Waals soft wall characterized by a 12-6 Lennard-Jones potential. The wall was set to a fixed buffer distance of 2.5 Å outside the specified radius of 12 Å. This value was optimized after several tests to probe the role of the size of the radius sphere. All molecular dynamics simulations were carried out with the TINKER software package[30] at 300 K with a 1 fs time step, for a total simulated time of 1 ns per trajectory. Configurations were recorded every 0.1 ps. Some preliminary tests performed with a small cluster containing 60 water molecules did not show strong structural difference, but the residence time in the first solvation shell was affected due to an uncomplete second shell. We chose the large cluster with 120 water molecules in order to pursue further studies where the gadolinium ion will be complexed with an organic molecule, that needing a large number of water molecules in order to be more fully solvated.

III- Structure and dynamics of the solvated ion

Table 1 lists the important results coming from an analysis of the molecular dynamics trajectories of the solvated Gd^{3+} ion. The standard error is provided by a small statistical set of five independent trajectories. Since all the errors are very small, we can consider that these structural and dynamical data are stable and reasonably converged.

a. Structural results

The radial distribution function g(r) for Gd-O pairs and the integrated curve are plotted in Figure 1. A narrow first peak observed at 2.44 Å indicates the location of the first coordination sphere. The integration of this peak gives a statistically averaged coordination number (CN) of 8.6. A second sphere is observed, more disordered than the first, with a larger peak centered at 4.65 Å, which corresponds to about 18 water molecules. Beyond this distance, no specific geometric arrangement can be pointed out anymore. These molecular dynamics results compare well with available experimental data such as EXAFS and X-ray diffraction studies, which bound the coordination number between 7.5 and 9.9 with large uncertainties.[31] The statistical value obtained here for this ion located in the middle of the lanthanide series is consistent as it is admitted that the coordination number decreases from 9 to 8 occurs along the series.[32] The experimental value of the Gd-O distances in the first coordination sphere ranges from 2.37–2.41 Å [Ref. 31] at coordination 8 to 2.40–2.55 Å [Ref. 33] at coordination 9. Concerning the second coordination sphere, no experimental data is available but our results suggest that it contains about 18 water molecules.

Figure 2 shows the distribution of the cosines of the angle between the HOH bisector and the Gd-O axis for both the first and second shells. This angle is generally small for all water molecules: lower than 20° for the first shell and lower than 25° for the second shell. A strong radial alignment is obtained which confirms the strong influence of the ion on the two first shells. Data extracted directly from molecular dynamics trajectories are quite noisy, and we use the short time average (STA) to reduce their fluctuations. The distribution of the short-time averaged coordination number over a period of 40 fs is plotted in Figure 3. A bimodal behavior consisting essentially of coordination numbers of 8 or 9 is clearly observed, the intermediate, non-integer values being

the result of the STA procedure. The dynamical aspects of the coordination number will be discussed below.

b. Evaluation of the residence time

The residence time of a water molecule inside the first hydration shell has been determined following Impey *et al.* who introduced the notion of persisting coordination.[33] This quantity is correlated to the persistence of a water molecule in the first hydration shell within a time t. However, temporary excursions are allowed provided they last less than t*, the latter quantity being commonly taken as 2 ps.[33] The residence time τ is determined by fitting a decay function *f(t)* that represents the distribution of the persistence time:

$$f(t) = n_{ion}^{0} \exp\left[-\left(\Gamma(1+\beta^{-1})t/\tau\right)^{\beta}\right] \quad (6).$$

In this equation Γ is the Euler gamma function and n_{ion}^{0} the statistical coordination number. β and τ are obtained from the fit, giving a residence time of the water molecules in the first shell of 372 ps (the value of β is about 1.4). This value is comparable to the ^{17}O NMR value of 833 ps obtained by Helm and Merbach[34] (the uncertainty of these measures on Gd^{3+} complexes is ± 20% [ref. 2]).

The motion of water molecules between the first and second hydration spheres of Gd^{3+} can be recognized from plotting the instantaneous Gd-O distances as a function of simulation time (see Figure 4a). Several water exchange processes are seen to occur within the total simulation time of 1 ns. An analysis of the trajectory gives an equilibrium value of the coordination number between 9 and 8 (63% for CN=9 and 37% for CN=8) with a preferred arrangement for coordination 9. We notice that no arrangement with CN=10 is ever observed in our simulations. Therefore, this result highlights a coexistence of associative and dissociative pathways for the water exchange mechanism. In Figure 5, the distribution of the time spent in coordination numbers 8 and 9, obtained from short time averages, is plotted. The data are accumulated from the five trajectories. The two average times are different and the average time spent at coordination 9 is significantly

longer than the one spent at coordination 8. This time can be correlated to the duration of the exchange phenomenon, which indicates that conformations with 8 water molecules in the first shell behave as an intermediate species.

IV- Charge transfer

a. Ab initio calculations

Ab initio Mulliken charges were calculated at QCISD level for the $[Gd(H_2O)_n]^{3+}$ clusters containing n=1, 2, or 4 water molecules and for gas-phase H_2O. For the cluster with n=8 molecules, we had to restrict to the MP2 level of computation. The QCISD level is the most accurate post-Hartree-Fock method available to calculate Mulliken charges using a core-polarization potential coupled to the large core ECP for Gd^{3+}. Table 2 gives the gadolinium and oxygen charges, as well as Δq, the partial charge transferred to Gd. The charge transfer to Gd is significant and grows roughly linearly from 1 to 8 water molecules surrounding the ion in the gas phase. The *ab initio* charges were used to fit the parameters of the fluctuating charges model for each atom type using a standard error minimization procedure.

b. Fluctuating charges models

At the level of electronic structure calculations, the determination of charge transfer between the lanthanide ion and the water molecules is no longer feasible for the large clusters considered in the AMOEBA simulations. The molecular dynamics trajectories have thus been analyzed with a fluc-q model. Our implementation of fluctuating charges is standard, and consists of attributing each chemical element (H, O, Gd) its electronegativity χ_i and hardness H_i. Since the fluc-q model is used for post-processing only, we have not considered more sophisticated continuous charge distributions as in the electronegativity equalization formalism of Rappé and Goddard.[11] At a given nuclear configuration $\boldsymbol{R}$, the charges $\{q_i\}$ carried by all atoms are determined to minimize the

global electrostatic energy $V_Q(\boldsymbol{R})$ under the constraint that the total charge of the system is kept fixed to a value $Q = \sum_i q_i$. V_Q is truncated at second order with respect to the charges:

$$V_Q(\mathrm{R}) = \sum_i \chi_i q_i + \sum_i \frac{1}{2} H_i q_i^2 + \sum_{i<j} J_{ij}(\mathrm{R}) q_i q_j + \lambda(Q - \sum_i q_i) \quad (7),$$

where λ is a Lagrange multiplier and $J_{ij}(\boldsymbol{R})$ only depends on the interatomic distance r_{ij} between particles i and j. Beyond this basic implementation of fluctuating charges, different constraints can be imposed to the system by including the appropriate Lagrange multipliers. The direct charge transfer between gadolinium and water can be removed by not including the charge on the ion in the last term of Eq. (7). Charge transfer will occur only within each molecule, but under the influence of the entire system, if the charge over each molecule is constrained to be neutral, which implies as many constraints. For these two types of constraints, the charge on gadolinium is set to +3 and only the charge on O and H atoms are allowed to vary.

Among the many possible forms for the electrostatic interactions, we chose a simple phenomenological expression:

$$J_{ij}(r) = (r_{ij}^3 + U_{ij}^{-3})^{-1/3} \quad (8).$$

When $i = j$, U_{ij} is taken as $H_i = H_j$. Otherwise, the empirical combination rule $U_{ij} = (H_i + H_j)/2$ is employed. The form above correctly behaves as $1/r$ at large r, and continuously tends toward U_{ij} for $r \to 0$. In addition, and contrary to the form used in Ref. 15, J_{ij} is always monotonically decreasing with r, thus preventing artefacts at intermediate or short distances. The minimization of V_Q with respect to the charges is carried out using standard linear algebra. The present model has only 5 independent parameters, namely the relative electronegativities of oxygen and gadolinium (hydrogen being taken as reference), as well as the three hardnesses of each element. These parameters have been fitted to reproduce the *ab initio* data on small clusters (with a RMS of 0.002) and the values obtained are 0.79 eV and 0.27 eV for the electronegativities of oxygen and

gadolinium, respectively, and 1.96 eV, 0.13 eV and 0.78 eV for the hardnesses of oxygen, gadolinium and hydrogen, respectively.

c. Analysis of molecular dynamics simulations

The fluc-q model was applied to each water-gadolinium configurations obtained from the molecular dynamics simulations. Due to the simplified character of this model and the possible inaccuracies in the reference Mulliken charges, the partial charges obtained and discussed bellow should be considered cautiously as semi-quantitative. Figure 4b-c shows the time evolution of the coordination number and the charge carried by the gadolinium ion obtained from short-time averages over the same 40 ps delay. A strong correlation between the bimodal behaviors of the two properties is observed. The charge lower than +1.9 corresponds to coordination 9, which is the arrangement most frequently found. Conversely the charge of about +2.0 corresponds to conformations with coordination number 8. This correlation is best seen when water exchanges between the first and second coordination shell take place, as the charge on gadolinium then undergoes its most dramatic variations. Figure 6 represents the distribution of the short-time averaged gadolinium charge, sorting the data according to the coordination number of the corresponding configurations. The bimodal character of the coordination number is strongly reflected in this figure. More importantly, the distributions obtained for the two coordination numbers do not overlap with each other. Therefore the relation between charge and coordination is unambiguous, which further supports our interpretation that two distinct stable species with coordination 8 and 9 in their first solvation shell coexist dynamically.

The charge on gadolinium averaged over all trajectories is evaluated to be $+1.91 \pm 0.15$ from the statistical set of configurations. Even though the present treatment of charge transfer is approximate, the present results show that the charge transferred from water to the gadolinium ion is significant and should not be underestimated. We can reasonably consider that about 1 electron is transferred to the ion, confirming that its interaction with water molecules is strong. A large part

of the fluctuation of 0.15 electrons comes from the coexisting species at coordination 8 and 9. However within one of these two species the fluctuations decrease down to less than 0.1 electrons. Therefore the chemical environment remains reasonably the same around the ion as long as its coordination does not change. Interestingly the average gadolinium charge transfer is lower than in the $[Gd(H_2O)_8]^{3+}$ cluster. This indicates that charge transfer is moderated by the environment, mainly by the second coordination shell. More specifically the influence of the second coordination shell was studied by analyzing the charge transfer induced by molecules from the first shell only, without considering farther molecules. The average charge was evaluated in this case to 1.6 ± 0.1, much closer to the *ab initio* Gd charge for the $[Gd(H_2O)_8]^{3+}$ cluster.

The variations of the charge carried by oxygen atoms provides extra information about the influence of the gadolinium ion on the solvent. In Figure 7 the average charge carried by oxygen atoms is represented as a function of the Gd-O distance. Here we employed the three different treatments of charge transfer among the solvated gadolinium ion that were aforementioned, namely with global CT between all atoms in the system, CT restricted to water molecules under the influence of the ion (no charge transferred to gadolinium), and no intermolecular CT (only intramolecular CT is allowed, each water molecule being globally neutral). In the last two approximations the solute is assumed to carry exactly the charge +3. The three different treatments allow us to quantify the effect of intermolecular charge transfer between water molecules and the influence of the gadolinium ion in separate ways.

The charge carried by oxygen atoms is maximum at the peak of the first coordination sphere (2.44 Å). It is obviously smaller when CT is allowed with gadolinium because the solute draws out some of these electrons. When the CT between Gd^{3+} and water molecules is neglected, the charge carried by oxygen is significantly larger, but does not change in large amounts if only intramolecular CT is allowed. Therefore in this case, the charge carried by oxygen is the result of intramolecular transfer mainly, perturbed by the Gd^{3+} solute. As can be seen from Figure 7, charge transfer remains non negligible at the second coordination sphere and should not be overlooked.

Our results clearly show that in the second sphere the influence of the ion and the transfer between water molecules are of comparable magnitude, with respect to the isolated molecule (-0.55 on oxygen).

V- Conclusions

The present *ab initio* and molecular dynamics study of the gadolinium (III) ion hydration was performed using a variety of methods, in an effort to achieve atomistic simulations over relatively long time scales and involving the solvent explicitly. A high level model potential that includes essential polarization effects was chosen, based on the AMOEBA force field developed by Ren and Ponder.[7] The parameters required for the gadolinium-water interactions were fitted on CCSD(T) / LC+CPP electronic structure calculations on the Gd^{3+}-H_2O dimer without introducing any experimental data, in the same spirit as in the original AMOEBA framework. The results obtained from analyzing the molecular dynamics trajectories are in good agreement with available experimental data for both the structural data of the first coordination shells and the residence time of a water molecule in the first coordination shell. Moreover, new information have been provided, such as the geometric arrangement of the second coordination shell and the coexistence of associative and dissociative pathways during water exchanges.

A fluctuating charges model was implemented as a tool of analysis of trajectory post-treatment in order to estimate the charge transfer effects in the hydration process. Again, the fluc-q model was parameterized on *ab initio* calculations performed on a small set of $[Gd(H_2O)_n]^{3+}$ clusters. Despite its relative simplicity, this model provides semi-quantitative data on charge transfer in large systems for which electronic structure calculations would have been prohibitive. In particular it allows us to correlate trends between charge transfer and the coordination number in the statistical context of molecular dynamics simulations. A significant charge transfer from the water molecules to the gadolinium ion was found, exceeding one electron. Strong correlations between the bimodal behaviors of the gadolinium charge, the coordination number and the time spent in each of the

two coordinations were established. These results show the coexistence of two stable chemical species with either 8 or 9 water molecules surrounding the ion in the first coordination sphere, which are characterized by different charges carried by the solute, as well as different residence times. We can conclude that in lanthanide compounds many-body effects are important and characterized not only by polarization but also by charge transfer phenomenon. In order to model many-body effects more accurately, a second step should be an improvement of the force field incorporating fluctuating charges and dipoles.

The present study encourages us to go on with more complex systems by introducing an organic ligand in the first coordination sphere of the gadolinium ion. This ligand should be selected in the contrast agent family of polyaminocarboxylates recognized for their efficiency in MRI applications.

Acknowledgments

This work was supported by EMIL European Network of Excellence (Sixth Framework Program). J.P.D. & C.C. thank the direction of simulation and experimental tools of the CEA nuclear energy division (CEA/DEN/DSOE) for financial support.

References

[1] A. E. Merbach and E. Toth, *The Chemistry of Contrast Agents in Medical Magnetic Resonance Imaging*. (Eds. John Wiley & Sons, Chichester, 2001).

[2] L. Helm and A. E. Merbach, Chem. Rev. **105**, 1923 (2005).

[3] T. Kowall, F. Floglia, L. Helm, and A. E. Merbach, J. Am. Chem. Soc. **117**, 3790 (1995).

[4] F. M. Floris and A. Tani, J. Chem. Phys. **115**, 4750 (2001).

[5] C. Clavaguéra, R. Pollet, J. M. Soudan, V. Brenner, and J. P. Dognon, J. Phys. Chem. B **109**, 7614 (2005).

[6] A. Grossfield, J. W. Ponder, and P. Y. Ren, J. Am. Chem. Soc. **125**, 15671 (2003).

[7] P. Y. Ren and J. W. Ponder, J. Phys. Chem. B **107**, 5933 (2003).

[8] P. Y. Ren and J. W. Ponder, J. Comput. Chem. **23**, 1497 (2002).

[9] L. Tůma, D. Jeníček, and P. Jungwirth, Chem. Phys. Lett. **411**, 70 (2005).

[10] W. J. Mortier, K. V. Genechten, and J. Gasteiger, J. Am. Chem. Soc. **107**, 829 (1985).

[11] A. M. Rappé and W. A. Goddard III, J. Phys. Chem. **95**, 3358 (1991).

[12] S. W. Rick, S. J. Stuart, and B. J. Berne, J. Chem. Phys. **101**, 6141 (1994).

[13] S. W. Rick, S. J. Stuart, and B. J. Berne, J. Chem. Phys. **117**, 266 (2002).

[14] F. H. Streitz and J. W. Mintmire, Phys. Rev. B **50**, 11996 (1994).

[15] J. Roques, F. Calvo, F. Spiegelman, and C. Mijoule, Phys. Rev. Lett. **90**, 075505 (2003); J. Roques, F. Calvo, F. Spiegelman, and C. Mijoule, Phys. Rev. B **68**, 205412 (2003).

[16] S. Patel, A. D. Mackerell Jr., and C. L. Brooks III, J. Comput. Chem. **25**, 1504 (2004).

[17] A. C. T. van Duin, S. Dasgupta, F. Lorant, and W. A. Goddard, J. Phys. Chem. A **105**, 9396 (2001).

[18] D. M. York and W. Yang, J. Chem. Phys. **104**, 159 (1996).

[19] R. T. Sanderson, Science **114**, 670 (1951).

[20] A. J. Stone, GDMA 13 (University of Cambridge, 2003).

[21] B. T. Thole, Chem. Phys. **59**, 341 (1981).

[22] T. A. Halgren, J. Am. Chem. Soc. **114**, 7827 (1992).

[23] N. L. Allinger, Y. H. Yuh, and J. H. Lii, J. Am. Chem. Soc. **111**, 8551 (1989).

[24] C. Clavaguéra, T. Saue, and J. P. Dognon, to be published.

[25] C. Clavaguéra and J. P. Dognon, Chem. Phys. **311**, 169 (2005).

[26] C. Clavaguéra, V. Brenner, S. Hoyau, C. J. Marsden, P. Millié, and J. P. Dognon, J. Phys. Chem. B **107**, 3051 (2003).

[27] H. Grubmüller, *SOLVATE 1.0.* (http://www.mpibpc.mpg.de/groups/grubmueller/start/index.html, 1996).

[28] D. Beeman, J. Comput. Phys. **20**, 130 (1976).

[29] H. J. C. Berendsen, J. P. M. Postma, W. F. v. Gunsteren, A. DiNola, and J. R. Haak, J. Chem. Phys. **81**, 3684 (1984).

[30] J. W. Ponder, TINKER - Software Tools for Molecular Desing - Version 4.2 (2004).

[31] T. Ohtaki and T. Radnal, Chem. Rev. **93**, 1157 (1993).

[32] S. Durand, J. P. Dognon, P. Guilbaud, C. Rabbe, and G. Wipff, J. Chem. Soc., Perkin Trans. 2, 705 (2000).

[33] R. W. Impey, P. A. Madden, and I. R. McDonald, J. Phys. Chem. **87**, 5071 (1983).

[34] L. Helm and A. E. Merbach, J. Chem. Soc., Dalton Trans., 633 (2002).

Table 1: Molecular dynamics results and their standard deviations for the Gd^{3+} - water cluster.

Average CN (1^{st} shell)	8.62 ± 0.02
Gd^{3+}-O distance in 1^{st} shell	2.44 ± 0.01 Å
%CN= 9 / 8	63% / 37% ± 2%
Number of H_2O in 2^{nd} shell	18.1 ± 0.2
Gd^{3+}-O distance in 2^{nd} shell	4.65 ± 0.01 Å
Residence time in 1^{st} shell	372 ± 12 ps

Table 2: Ab initio Mulliken charges for the $[Gd(H_2O)_n]^{3+}$ clusters.

	q(Gd)	$\Delta q/H_2O$	q(O)
$Gd^{3+}(H_2O)$	+2.75	0.25	-0.63
$Gd^{3+}(H_2O)_2$	+2.54	0.23	-0.65
$Gd^{3+}(H_2O)_4$	+2.21	0.20	-0.62
$Gd^{3+}(H_2O)_8$	+1.58	0.18	-0.59

List of figure captions

Figure 1: Radial distribution function (RDF) $g(r)$ and integrated curve.

Figure 2: Probability distribution of the cosines of the tilt angle (between the HOH bisector and the Gd-O axis) for the water molecules in the first and second coordination shells.

Figure 3: Probability distribution of the short-time averaged coordination number of Gd^{3+}.

Figure 4: Time evolution of the short-time averaged Gd-O distance (a), coordination number (b) and gadolinium charge (c).

Figure 5: Probability distribution of the short-time averaged persistence time in coordination 8 (in black bars) and 9 (in grey bars).

Figure 6: Probability distribution of the short-time averaged gadolinium charge after the fluctuating charge treatment.

Figure 7: Variation of the average oxygen charge as a function of the Gd-O distance obtained from 3 different fluc-q models (see text for details).

Figure 1:

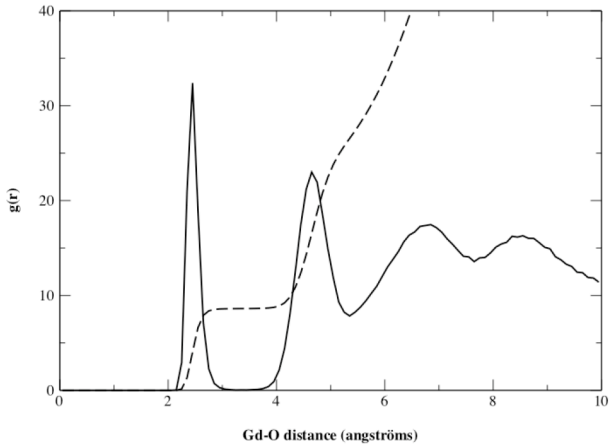

Figure 2:

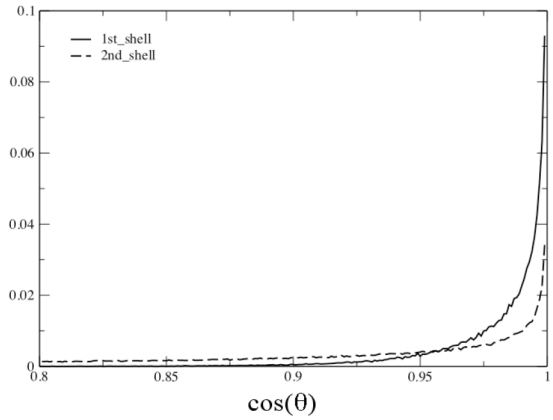

Figure 3:

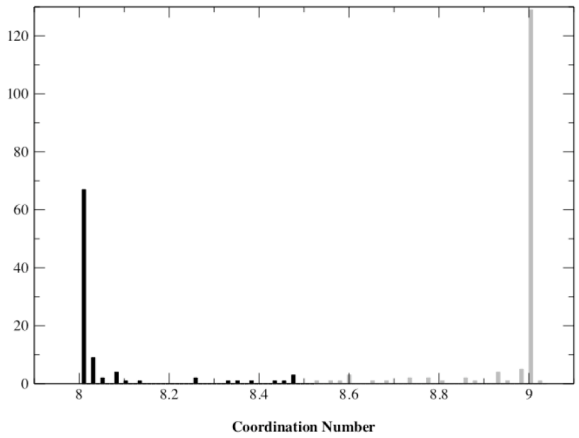

Figure 4:

a

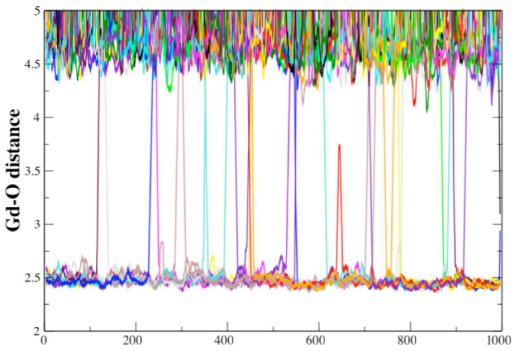
Gd-O distance
5
4.5
4
3.5
3
2.5
2
0
200
400
600
800
1000

b

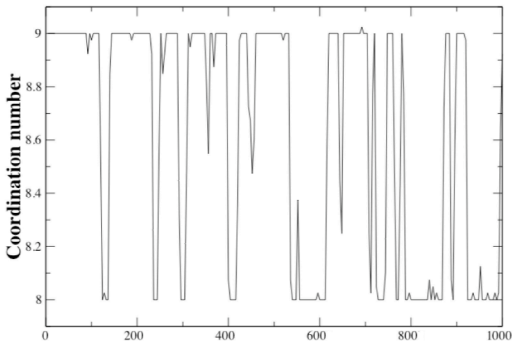
Coordination number
9
8.8
8.6
8.4
8.2
8
0
200
400
600
800
1000

c

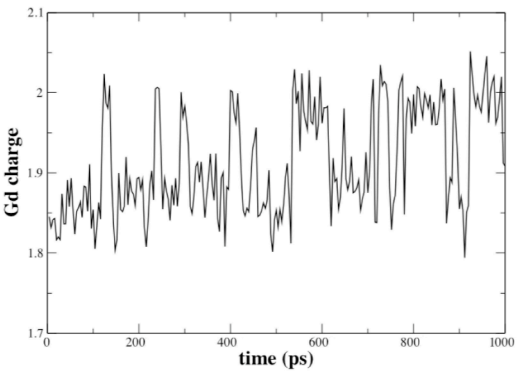
Gd charge
2.1
2
1.9
1.8
1.7
0
200
400
600
800
1000
time (ps)

Figure 5:

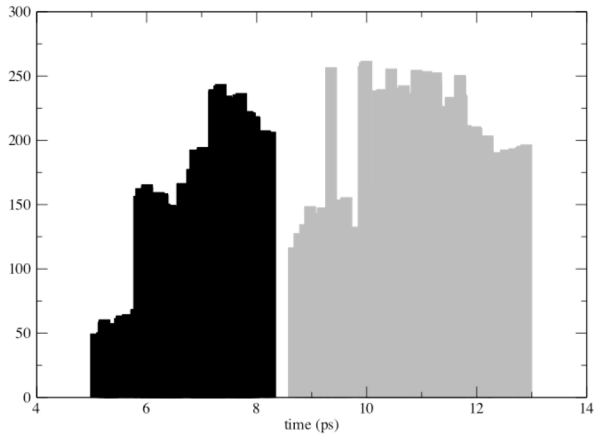

Figure 6:

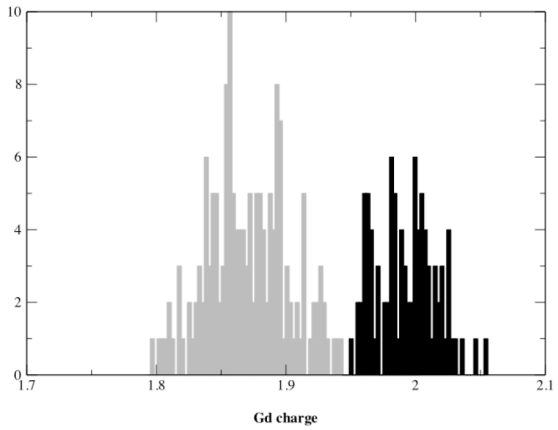

Figure 7:

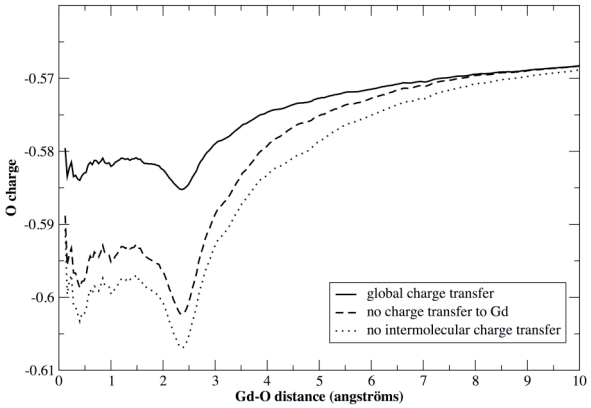
-0.57
-0.58
-0.59
-0.6
-0.61
O charge
0
1
2
3
4
5
6
7
8
9
10
Gd-O distance (angströms)
global charge transfer
no charge transfer to Gd
no intermolecular charge transfer